Mathematical modelling of a hydraulic controller for PRV flow modulation

Hossam AbdelMeguid, Piotr Skworcow and Bogumil Ulanicki

ABSTRACT

This paper describes the development of mathematical models, which represent static and dynamic properties of the AQUAI-MOD® hydraulic controller coupled with a standard pressure reducing valve (PRV) as well as a new experimental set-up for testing the controller and calibrating and validating the models. The purpose of the AQUAI-MOD® controller is to modulate the PRV outlet pressure according to the valve flow. The controller has been experimentally tested to assess its operation in different conditions and operating ranges and in all cases showed good performance. The mathematical models of the PRV and its controller have been developed and solved using the Mathematica software package to represent both steady state and dynamics conditions. The numerical results of simulation of the mathematical model have been compared with experimental data and showed a good agreement in magnitude and trends. The model can be used to simulate the behaviour of the PRV and the AQUAI-MOD® hydraulic controller in typical network applications. It can also be used at the design stage to size the controller components and to compute the required set points for the minimum and the maximum pressure before installing the controller in the field.

Key words | flow-modulation, hydraulic controller, laboratory test, mathematical model, pressure control, PRV

Hossam AbdelMeguid (corresponding author)
Piotr Skworcow
Bogumil Ulanicki
Process Control – Water Software Systems,
Faculty of Technology,
De Montfort University Hawthorn Building, (00.26),
The Gateway,
Leicester, LE1 9BH,
UK
E-mail: *hssaleh@gmail.com*

ABBREVIATION AND NOTATION

a_1	Bottom area of the moving element of the PRV	Cv_{ma}	Discharge capacitance of the modulation adjuster
a_2	Top areas of the moving element of the PRV	Cv_{mv}	Discharge capacitance of the PRV
A_1	Internal cross sectional area of the large cylinder of the controller	Cv_{nv}	Discharge capacitance of the bi-directional needle valve
A_2	Internal cross sectional area of the small cylinder of the controller	D_4	Diameter of the connecting pipe between the Pitot tube and T-junction ($t2$)
A_4	Internal cross sectional area of the connecting pipe between the Pitot tube and T-junction ($t2$)	f_4	Friction coefficient of the connecting pipe between the Pitot tube and T-junction ($t2$)
A_j	Discharge area of the jet	f_m	Friction coefficient of the moving element of the PRV
$A_{mv,out}$	Cross sectional area of the PRV outlet		
A_{Pitot}	Cross sectional area of the Pitot tube	f_{sh1}	Friction coefficient of the modulation shaft
Cv_{fo}	Discharge capacitance of the fixed orifice		
Cv_j	Discharge capacitance of the pilot valve	f_{sh2}	Friction coefficient of the pilot shaft

g	Gravitational acceleration
h_{cc}	Pressure in the control chamber of the controller
h_{cj}	Pressure in the jet chamber of the controller
h_{cpt}	Pressure of the Pitot chamber of the controller
h_{in}	PRV inlet pressure
h_{out}	PRV outlet pressure
$h_{out,t}$	Total pressure at the PRV outlet
h_{t1}	Pressure at the T-junction ($t1$)
h_{t2}	Pressure at the T-junction ($t2$)
h_{vc}	Pressure in the PRV control space
k_{sp1}	Stiffness coefficient of the springs on the modulating shaft
k_{sp2}	Stiffness coefficient of the springs on the pilot shaft
L_4	Length of the connecting pipe between the Pitot tube and T-junction ($t2$)
$L_{c1,2}$	Length of the fixed section of the controller
L_{c3}	Length of the variable section of the controller (main pressure adjuster)
L_{sh1}	Length of the modulation shaft
L_{sh2}	Length of the pilot shaft
m_m	Mass of the moving element of the PRV
m_{sh1}	Mass of the modulation shaft
m_{sh2}	Mass of the pilot shaft
n	Number of opening turns of a valve
N_{mpadj}	Number of opening turns of the main pressure adjuster
PRV	Pressure reducing valve
q_1	Flow from the PRV inlet to the T-junction ($t1$)
q_2	Flow from the control space of the PRV to T-junction ($t1$)
q_3	Flow from/to the valve control space through the bi-directional needle valve
$q_{3,sat}$	Saturation flow of the bi-directional needle valve
q_4	Flow through the Pitot tube
q_5	Flow from/to the Pitot chamber of the controller
q_6	Flow through the modulation adjuster
q_m	Main flow through the PRV
$t1$	T-junction 1
$t2$	T-junction 2
x_m	Displacement of the moving element of the PRV
x_r	Gap between the jet and the seat of the pilot valve
x_{sh1}	Displacement of the modulation shaft
x_{sh2}	Displacement of the pilot shaft
Δh	Pressure loss across the element
β_1, β_2	Coefficients of a convex combination of the inlet and outlet pressures
$\beta_{1,\text{critical}}$	Value of β_1 at which the model is singular
ρ	Density of water

INTRODUCTION

Water utilities use pressure control to reduce background leakage and the incidence of pipe bursts. Significant savings can often be made and there are many examples where the application of pressure control has been extremely successful (Rogers 2005; Marunga *et al.* 2006; Çakmakcı *et al.* 2007; Girard & Stewart 2007; Yates & MacDonald 2007). The control is usually implemented across areas that are supplied through pressure reducing valves and closed at all other boundaries, and known as districted metered areas (DMAs) (Alonso *et al.* 2000; Ulanicki *et al.* 2000; Prescott *et al.* 2005). Single-feed pressure reducing valve (PRV) schemes are often adopted for ease of control and monitoring but risk supply interruption in the event of failure. Multi-feed systems improve the security of the supply but are more complex and incur the risk of PRV interactions leading to instability (Ulanicki *et al.* 2000; Prescott & Ulanicki 2004).

PRV can be fixed set-point, dual set-point or fully modulated. A fixed set-point PRV is a standard pressure reducing valve that regulates a high varying upstream pressure to a lower fixed and stable downstream pressure regardless of variations in demand flow. The set-point of the fixed outlet PRV is manually set so that the pressure at the critical node is higher than the minimum value as required by the local regulations. Dual set-point PRV regulates the outlet pressure to two different values according to the time of the day or the demand flow. The high set-point is selected in the same manner as in the fixed set-point PRV, while the lower setting point is adjusted considering the lower system friction losses correlating to the low demand flow. The application of this valve achieves better leakage reduction compared with the fixed set-point PRV. However, the pressure at the critical node may still be too high if the demand flow is lower than the maximum demand but not sufficiently low to switch to

the low-pressure setting. Therefore, the classical usage for dual set-point PRV would be in locations where there is a distinct difference between the normal demand flow and the low demand flow, such as in the case of a PRV supplying a DMA with normal domestic demand and a single large industrial customer which causes a significant flow increase. The fully modulated PRV regulates the outlet pressure to varying set-points, so that the pressure at the critical node remains fixed at the minimum allowed pressure and stable regardless of friction loss variations due to demand flow. The set-points can be modulated according to either demand flow, time of the day or current value of pressure at the critical node, which is sent via telemetry system to the PRV controller. This type of operation enables a maximum optimization of leakage reduction, with the best level of customer service, as the pressure is kept stable regardless of demand variations. Fully modulated PRVs are usually controlled by an electronic controller that monitors the pressures and/or the demand flow rate and modifies the set-point of the pilot valve of a standard PRV.

During the implementation of a pressure control scheme, both steady state and dynamic aspects should be considered (Brunone & Morelli 1999; Ulanicki *et al.* 2000; Prescott & Ulanicki 2003, 2008). The steady state aspects ensure that PRV set-points are changed according to the demand flow to minimize background leakage and to satisfy the minimum required pressure at the critical nodes. The dynamic aspect considers preventing excessive pressure hunting (oscillations) across a network caused by interactions between modulating valves and dynamics in a water network. A better understanding of the dynamics of PRVs and networks will lead to improved control strategies and reduced instabilities and leakage. Dynamic models are currently available for representing the behaviour of most water network components. Such models are relatively simple, accurate and can be easily solved (Pérez *et al.* 1993; Andersen & Powell 1999; Brunone & Morelli 1999). In Prescott & Ulanicki (2003) PRV dynamic phenomenological, behavioural and linear models to represent dynamic and transient behaviour of PRVs were developed, while in (Prescott & Ulanicki 2008) a model to investigate the interaction between PRVs and water network transients was described; transient pipe network models incorporating random demand were combined with a behavioural PRV model to demonstrate that

sudden changes in the system demand can produce large and persistent pressure variations, similar to those seen in practical experiments.

Pressure control is more efficient if there is a possibility of automatically adjusting the set point of a PRV according to the PRV flow – so called flow modulation. The PRV set point can be adjusted electronically or hydraulically. The former requires the use of a flow sensor, a microcontroller and solenoid valves acting as actuators. The major disadvantage of this solution is the necessity of providing electrical power supply and the exposure of the electronic equipment to harsh field conditions. A hydraulic flow modulator is a simpler solution and is considered to be more robust than an electronic controller. The AQUAI-MOD® hydraulic controller manufactured by Aquavent (Peterborough, UK) is probably the first hydraulic flow modulator available on the market.

The AQUAI-MOD® hydraulic controller can be used to implement optimal pressure control strategies which have been developed earlier and described in Vairavamoorthy & Lumbers (1998) and Ulanicki *et al.* (2008) by modulating the outlet pressure of the PRVs according to the flow. Such an approach minimises continuous over pressurisation and stress on the mains which extends infrastructure life, and therefore reduces leakage and subsequently reduces energy consumption by pumping a smaller volume of water (Thornton & Lambert 2007; Colombo & Karney 2009).

The main aim of this paper is to develop a detailed mathematical model of the PRV and its controller based on the phenomenological concept of each element of the system. Such a model can be used to improve the design and mechanical construction of the controller, to resize its components, improve its robustness and functionality and to better understand the dynamics of the system to prevent the valve hunting. Another important aim is to show what modelling approach and applications were used, in order to facilitate other authors developing mathematical models of similar systems.

DESCRIPTION OF THE AQUAI-MOD® HYDRAULIC CONTROLLER

The AQUAI-MOD® hydraulic controller consists of three main chambers separated by rolling diaphragms, as shown in
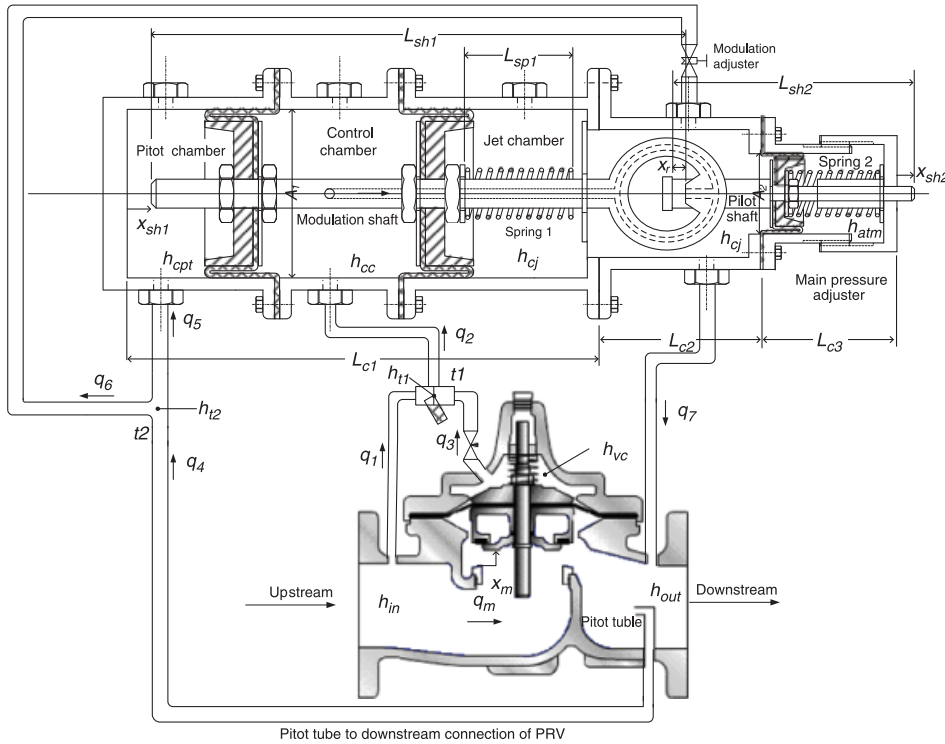
Figure 1 | AQUAI-MOD® controller and its connection to PRV (Patents Pending GB 0711413.5, Int'l PCT/GB2008/050445).

Figure 1. The first is the Pitot chamber, which is connected to the Pitot tube at the outlet of the PRV. The second is the control chamber, which is connected to the inlet and the control space of the PRV through T-junction, $t1$. The pipe connecting the valve inlet and $t1$ has a fixed orifice. The third is the jet chamber, which is connected to the outlet of the PRV. The jet chamber is also connected to the Pitot tube through T-junction, $t2$. The control chamber is connected to the jet chamber by a hollow shaft (the modulating shaft), which allows the flow from the control chamber to the jet chamber through the discharge outlet of the jet. The flow through the modulating shaft depends on the gap (x_r) between the jet exit and the seat of the pilot shaft, these arrangements work like a pilot valve of a standard PRV (Prescott & Ulanicki 2003). Note that the control chamber has a constant volume while the volume of the Pitot and jet chambers depends on the position of the modulating shaft connected to rolling diaphragms.

The controller modulates the outlet pressure of the PRV according to the main flow, which is sensed and converted to dynamic pressure by the Pitot tube. Standard installation of the controller requires the definition of two set points. The first one is the 'minimum pressure' (corresponding to the minimum night flow), which is adjusted by turning the main pressure adjuster that changes the initial tension of spring 2. The working principle of this part is similar to that of a traditional pilot valve in a PRV. The second set point is for the 'maximum pressure' (corresponding to the peak demand) which can be set by changing the opening of the modulation adjuster (one directional flow needle valve). If modulation adjuster valve is fully open, there is no flow modulation and the controller acts as a standard PRV pilot valve.

LABORATORY STUDIES

In this section the descriptions of the test rig, the experiments and the results of testing the PRV and the hydraulic controller in different operating conditions are presented. The experiments were performed in a physical test rig where the controller and PRV could be subjected to a wider range of operating conditions than those that could be achieved in a real network without affecting customers. The system comprising a PRV and hydraulic controller was tested to assess

and to evaluate the functionality and robustness of the system, evaluate its performance under a wide range of steady-state and dynamic operating conditions, and to use the experimental data to validate the developed mathematical model.

Test rig description

The test rig used for the experiments was a closed hydraulic loop illustrated in Figure 2. A centrifugal fixed speed pump delivers the water from the tank through a 3 inch stainless steel pipe which is expanded to a 4 inch pipe before the fitting of the gate valve. The hydraulic loop has two gate valves and a Claval NGE9001 PRV controlled by AQUAI-MOD® hydraulic controller. The first gate valve is upstream of the PRV and is used to control the PRV inlet pressure, while the second gate valve is downstream of the PRV and is used to control the main flow, which represents the demand flow. The 4 inch stainless steel pipe connects the upstream gate valve, the PRV, the downstream gate valve and finally exits to the tank.

Figure 2 depicts the detailed instrumentation drawing of the test rig and shows the position of each sensor and its connection to the data acquisition card. The test rig is equipped with two electromagnetic flow meters. One is a high-flow range flowmeter to measure the main flow and another is a low-flow range flowmeter, which can be installed in different positions, to measure the flow from $t1$ to the control chamber of the controller (Position 1) or to measure

the flow through the modulation adjuster (Position 2). Additionally, seven pressure transducers have been installed to measure the inlet and outlet pressures of the PRV; the pressures in the Pitot, control, and jet chambers of the controller; the pressure in the control space of the PRV; and finally the pressure at $t1$. A linear variable differential transducer (LVDT) was installed to measure the displacement of the modulating shaft of the controller. All transducers have 4–20 mA output signals to prevent electro-magnetic interference and the main flowmeter is connected via a RS232C link to the monitoring computer; the technical specifications of the transducers and flow meters are presented in Table 1. In order to automate the data collection, a NI 9203 series data acquisition card (DAQ) with 16 high accuracy analogue input channels, was used to collect different signals from the measurement transducers. A LabView-based data acquisition software was installed on the laptop to monitor and record 10 samples of the acquired signals per second in CSV format.

TESTING BEHAVIOUR OF THE PRV WITH THE CONTROLLER IN DIFFERENT OPERATING CONDITIONS

Measuring flow modulation characteristic (test 1)

Using the main pressure adjuster of the controller, the minimum outlet pressure was set to 26 m. Measurements were
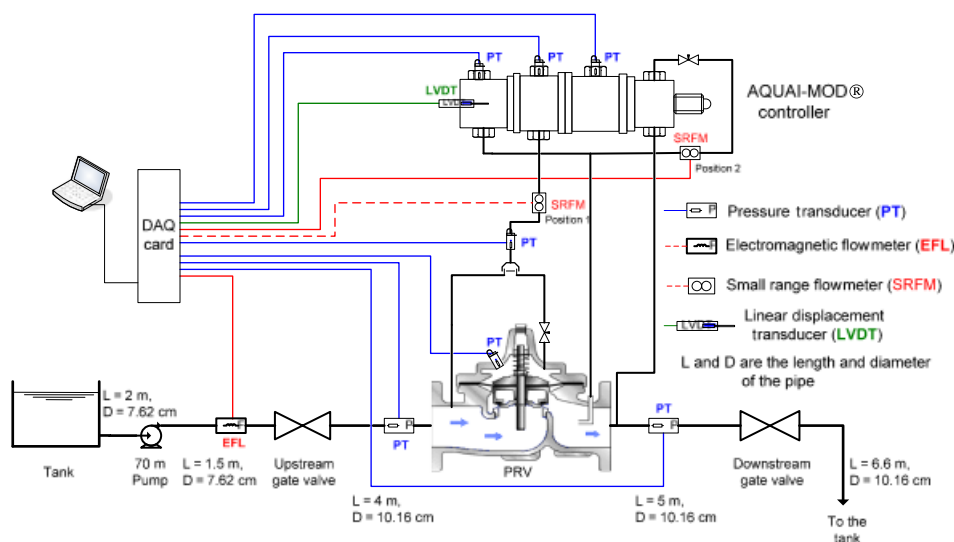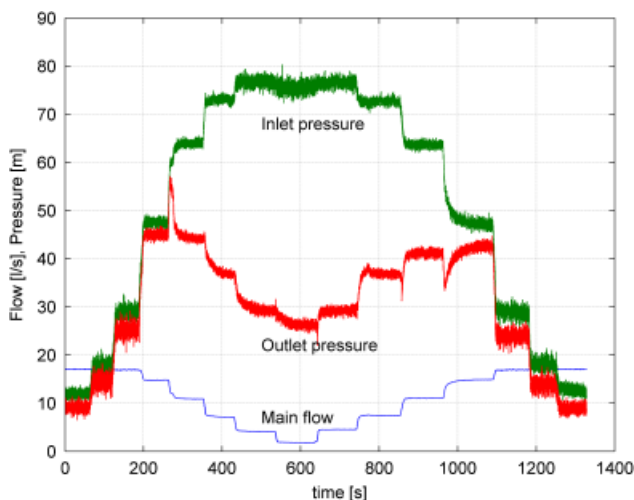

Figure 2 | AQUAI-MOD® hydraulic controller experiment layout.

Table 1 | Technical specifications and accuracies of the sensors and transducers

Sensor	Specifications
Electromagnetic Flowmeter	MagMaster – Water & Waste Water Version SS/MAG/WW
	Accuracy $<0.15\%$ over the operating range of the equipment
	From: ABB, website: www.abb.com
Low-range flowmeter	FMG230-NPT series flow meter. Range 0.0025–0.633 l/s, O/P 4–20 mA, accuracy 1% and hysteresis 6.25%
	From: OMEGA Engineering, INC, website: www.omega.com
Pressure Transducers	642 R series pressure transmitter. Range 0–10 bar, O/P 4–20 mA (2 wire), accuracy $<0.25\%$, with G1/4' BSP male process connection, and M12 electrical connector. Power supply 10–32 vDC.
	From: Omni Instruments, website: www.omniinstruments.co.uk
LVDT Transducers	Industrial LVDT Series AML/IEI $+/-12.5$. Stroke range: ±12.5 mm, O/P 4–20 mA (3 wire), non-linearity: $\pm0.50\%$
	From: Applied Measurements Limited, website: www.appmeas.co.uk

carried out for different modulation adjuster settings: from 0 to 80 per cent in 10 per cent steps. For each modulation adjuster setting the downstream gate valve opening was changed (according to the sequence 6, 5, 4, 3, 2.5, 2, 1.5, 1, 1.5, 2, 2.5, 3, 4, 5, 6 turns from the complete closure), so that the main flow varied over the range 1.75–17 l/s. Between each change of the downstream gate valve setting sufficient time was allowed (between 1 and 2 minutes) for the controller and the PRV to reach the steady-state conditions. Figure 3 shows the effect of the flow changes on the outlet pressure of the PRV. The flow and PRV inlet pressure are changing in a way similar to the actual operation of a water distribution system, when the flow decreases the pressure increases and vice versa. When the flow ranged from 15 to 17 l/s, the inlet pressure was too low due to the pump characteristics, therefore the PRV outlet pressure was not modulated and was lower than the inlet pressure due to the friction losses in the valve. When the flow ranged from 1.75 to 15 l/s the PRV outlet pressure was modulated according to the flow between the minimum and maximum setting of the controller; as the flow decreases the PRV outlet pressure decreases and vice versa. The measurements of the PRV coupled to the controller do not show any significant dynamic effects on the PRV outlet pressure due to the flow changes.

Changes of modulation adjuster setting (test 2)

The opening of the modulation adjuster valve was changed according to the sequence: 25, 30, 40, 50, 60, 70 and 80 per cent, respectively. Between each change of the modulation adjuster setting sufficient time was allowed (between 1 and 2 minutes) for the system to reach the steady-state conditions. Figure 4 depicts the effect of the modulation adjuster setting on the PRV outlet pressure. As the opening of the modulation adjuster valve increases the PRV outlet pressure decreases, which provides flexible controller setting of the PRV maximum outlet pressure to fit a wide range of operating conditions and demand flow patterns.
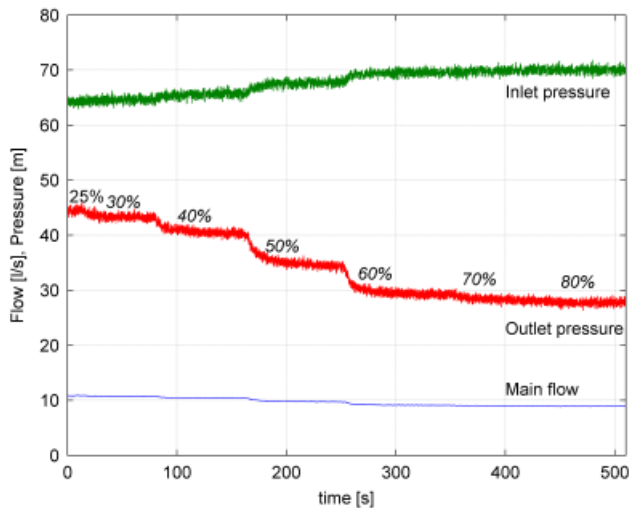

Figure 3 | Flow modulation of the PRV outlet pressure in a typical operating condition.

Figure 4 | Effect of modulation adjuster setting of the controller on the PRV outlet pressure.

Changes of the main pressure adjuster setting (test 3)

With the modulation adjuster set at 30 per cent, the minimum outlet pressure was changed every minute by turning the main pressure adjuster (one turn at a time). This was performed starting from the highest pressure setting towards the lowest pressure setting. Figure 5 illustrates the effect of main pressure adjuster setting, denoted N_{mpadj}, on the PRV outlet pressure. Changing the setting from one to three turns of the main pressure adjuster had no effect on the PRV outlet
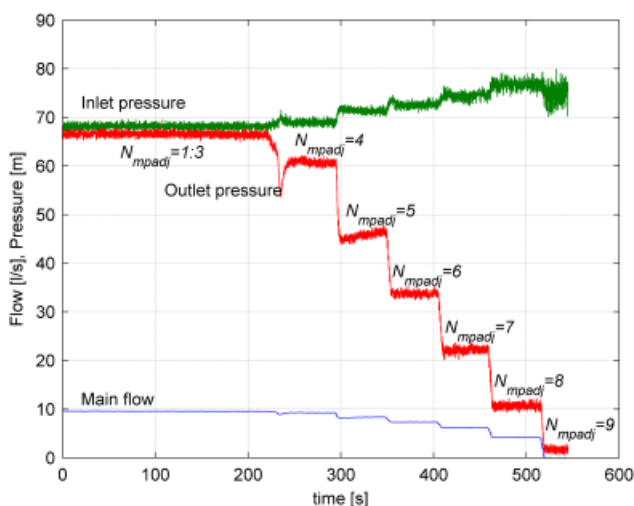
pressure, however changing the setting from four to eight turns decreased the PRV outlet pressure by 12 m per turn, which gives flexibility for the PRV minimum pressure setting to cope with different DMA characteristics and operating conditions.

Sharp closure and opening of the downstream gate valve (test 4)

With the modulation adjuster set at 30 per cent and the downstream gate valve set initially at six turns from complete closure, the downstream gate valve was sharply turned to almost complete closure (one turn away from the complete closure) in less than 15 s and after 2 minutes the downstream gate valve was sharply opened to the initial opening in less than 20 s. Figure 6 shows the results of test 4 where the effects of a sudden drop and subsequent rise in the main flow are displayed. By closing the downstream gate valve, the main flow decreased from 17 to 1.75 l/s in 15 s, and the outlet pressure dramatically increased to its maximum value of 77.5 m in 10 s and then dropped to its nominal value of 24.6 m. However, sharp opening of the downstream gate valve and hence rapid flow increase did not have such significant transient effect on the outlet pressure. The dynamic behaviour for each time interval in Figure 6 is explained below.

In interval (1) the main flow is high which causes the inlet pressure to be low due to the pump characteristic. The desired
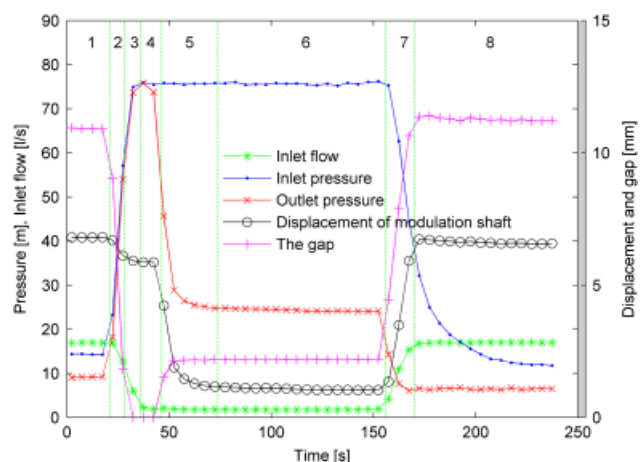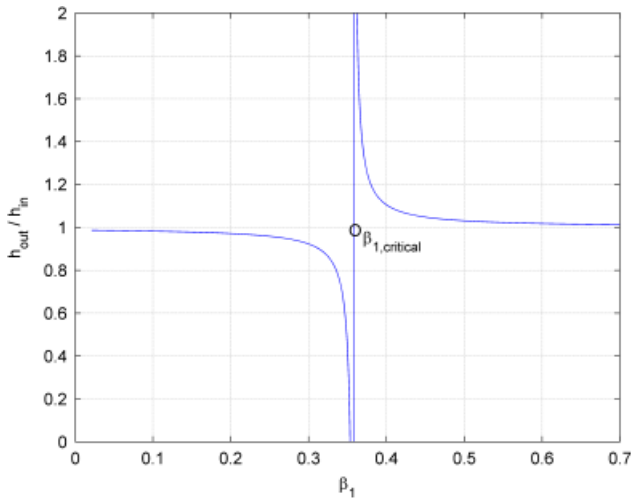

Figure 5 | Effect of main pressure adjuster setting of the controller on the PRV outlet pressure.

Figure 6 | Dynamic effect of quick drop and rise in the main flow.

Figure 7 | The solution of Equation (26) for a given inlet pressure and flow.

outlet pressure cannot be maintained and the PRV is almost fully open.

In interval (2) the main flow is decreasing and this has the following effects.

(a) The inlet pressure is increasing due to the pump characteristic.
(b) The PRV is still fully open and the outlet pressure is almost equal to the inlet pressure (increasing).
(c) The modulating shaft moves to the left because of decreasing dynamic pressure.
(d) The pilot shaft is moving to the right because of the increasing outlet pressure.

In interval (3) the main flow is still decreasing but: (a) the jet outlet of the modulating shaft is engaged with the seat of the pilot shaft thus the modulating shaft stops; and (b) the PRV is still fully open and the outlet pressure is almost equal to the inlet pressure (increasing).

In interval (4) the main flow is now constant and this has the following consequences.

(a) The inlet pressure is constant.
(b) The gap between the jet outlet and the seat of the pilot shaft is zero and the pressure in the control chamber and T-junction rapidly increases. This results in flow q_3 going into the control space of the PRV and forcing the main element of the PRV to move down, that is, the PRV is closing.

(c) The outlet pressure is decreasing and so is the pressure acting on the pilot shaft diaphragm.
(d) The pilot shaft moves very slowly to the left and so does the modulating shaft; both of them are still engaged.

In interval (5) the main flow is constant and the PRV and its controller undertakes normal operation.

(a) The main element of the PRV continues to move down (flow q_3 keeps going into the control space of the PRV).
(b) The outlet pressure is decreasing.
(c) The pilot shaft moves to the left and so does the modulating shaft driven by the spring; the gap between the jet outlet and the seat of the pilot shaft is close to zero.
(d) At the end of this period the steady-state is achieved: (i) the modulating shaft stops at the position where forces from the dynamic pressure and spring 1 are balanced; (ii) the pilot shaft stops at the position where forces from outlet pressure and spring 2 are balanced; (iii) the gap between the jet outlet and the seat of the pilot shaft is such that the pressure at T-junction equals the pressure in the PRV control space: flow q_3 is zero and the PRV stops closing.

In interval (6) the main flow is constant and the PRV and its controller are in steady state.

In interval (7) the main flow is increasing rapidly due to opening of the downstream gate valve and this causes the following.

(a) The modulating shaft moves to the right due to increase in the flow and resulting increase in the dynamic pressure; it stops when the dynamic pressure is balanced by the force of spring 1.
(b) The inlet and outlet pressures are decreasing rapidly due to the pump characteristic and so is the pressure acting on the pilot shaft diaphragm, hence the pilot shaft moves to the left.
(c) The gap between the jet outlet and the seat of the pilot shaft becomes large and has small resistance, therefore the pressure in the control chamber and T-junction rapidly decreases. This results in flow q_3 going out of the control space of the PRV and forces the main element of the PRV to move up, that is, the PRV is opening.

In interval (8) the main flow becomes constant and has a high value and the following occurs.

(a) The dynamic pressure is constant and the modulating shaft stops balanced by the force from the spring 1.

(b) The PRV is still opening trying to maintain the outlet pressure and subsequently the inlet pressure is decreasing due to distribution of the pressure between the upstream gate valve and the PRV.

(c) Finally the PRV and its controller reach steady state and the PRV is almost fully opened.

In the case of rapid decrease in the flow rate combined with rapid increase in the inlet pressure, the PRV is fully opened, and the outlet is the same as the inlet for a few seconds then the controller closes the valve to the desired outlet pressure. Such a situation should not arise during the normal operation of a water distribution system. In all other cases the flow modulates the outlet pressure smoothly to the desired values.

EXPERIMENTS TO IDENTIFY COMPONENT PARAMETERS

An approach for deriving a phenomenological model of the system was adopted as described in the section 'Mathematical Model Description'. Due to the lack of technical specification provided by the manufacturer, for some components the physical characteristics of each component (e.g. modulation valve, fixed orifice, etc.) were measured as described below and calibrated separately based on the best fit.

Measuring discharge capacitance of the modulation adjuster (test a)

A water tank was placed at the height of 1.5 m. The modulation adjuster valve was detached from the controller and installed on an elastic pipe. One end of the pipe was connected to the tank bottom and the other pipe end was positioned at different heights (40, 60, 80, 100 and 120 cm respectively) with respect to the water level in the tank in order to measure flow through the pipe for different pressure differences. The choice of pressure differences was consistent with the pressures in the Pitot and jet chambers of the controller observed during normal operating conditions.

Water was discharged from the water tank through the pipe and modulation adjuster valve into a measuring cylinder. Such an approach was adopted because the flow was too small to be measured with the available low-flow flowmeter and for this reason the flow through the pipe was calculated from the volume of the water discharged into the cylinder over a given period of time (approx 30 s). The measurements were carried out for all possible combinations of modulation valve openings (from 10 to 80 per cent in steps of 10 per cent) and of pressure differences (from 0.4 to 1.2 m in steps of 0.2 m).

Measuring the discharge capacitance of the pilot valve (test b)

Since the pilot valve could not be detached from the controller, its discharge capacitance was evaluated during normal operation of the controller. The low-flow flow meter was installed between $t1$ and the control chamber to measure flow, q_2, for different gaps, x_r, between the jet outlet and jet seat. Note that x_r cannot be directly manipulated during the valve operation. To force the changes in x_r the downstream gate valve opening was changed causing the main flow to vary from 1.75 to 17 l/s. This was carried out for different settings of the modulation valve, that is, for 30, 40, 50 and 60 per cent of maximum opening.

MATHEMATICAL MODEL DESCRIPTION

To provide a good understanding of the static and dynamic behaviour of the PRV and its AQUAI-MOD® hydraulic controller, a full phenomenological model has been developed. In the current study, the developed model does not include the effect of pressure waves (water hammer) in the pipes of the system. The phenomenological model developed by (Prescott & Ulanicki 2003) is used to model the behaviour of a standard PRV, while the mathematical model of the controller is developed here.

Three moving parts are considered; the first is the main element of the PRV with the other two being the modulating and pilot shafts of the controller, as depicted in Figure 1. The displacement of each moving part is described by a second order differential equation (Newton's II Law), Equation (1)

for the main element of the PRV, and Equations (2) and (3) for the modulating shaft and the pilot shaft of the controller, respectively.

$$m_m \ddot{x}_m = \rho g[h_{in}a_1 + h_{out}(a_2 - a_1) - h_{vc}a_2] - m_m g$$
$$- f_m \dot{x}_m + \rho \frac{q_m^2}{a_1} \tag{1}$$

$$m_{sh1} \ddot{x}_{sh1} = \rho g(h_{cpt} - h_{cj})A_1 - k_{sp1}x_{sh1} - f_{sh1}\dot{x}_{sh1} + \rho \frac{q_2^2}{A_j} \tag{2}$$

$$m_{sh2} \ddot{x}_{sh2} = \rho g h_{cj}A_2 - k_{sp2}x_{sh2} - f_{sh2}\dot{x}_{sh2} - \rho \frac{q_2^2}{A_j} \tag{3}$$

The scripts, m, x, f and h denote the mass in kilograms, the displacement in metres, the friction coefficient opposing the movement of the element in kg/s and the head in metres, respectively; k is the stiffness coefficient of the spring in kg/s^2; q_m, q_1 and q_2 are the main flow through the PRV, the flow from the PRV inlet to $t1$ and the flow from the control space of the PRV to $t1$ in m^3/s, respectively; a_1 and a_2 are the bottom and the top areas of the main element of the PRV in m^2, respectively; A_1, A_2 and A_j are the internal cross-sectional areas of the large and small cylinders of the controller and the discharge area of the jet in m^2, respectively; ρ and g are the density of water in kg/m^3 and the gravitational acceleration in m/s^2. The subscripts, m, $sh1$ and $sh2$ refer to the moving element of the PRV, the modulating and pilot shafts of the AQUAI-MOD® controller, respectively; *in* and *out* refer to the inlet and outlet of the PRV, and *vc* refers to the control space of the PRV; *cpt, cc* and *cj* refer to the Pitot chamber, control chamber and jet chamber of the controller, respectively; *sp1* and *sp2* denote the springs on the modulating and pilot shafts of the controller, respectively.

The PRV under consideration is diaphragm operated so the top area of the moving element changes with the opening of the valve according to the equation (Prescott & Ulanicki 2003)

$$a_2 = \frac{1}{3700(0.02732 - x_m)} \tag{4}$$

The force terms in Equation (1) are, from left to right: the inlet pressure acting on the base of the moving element, the outlet pressure acting on the region of the diaphragm around the top of the moving element, the control space pressure acting on the top of this diaphragm, the weight of the moving element, the friction acting on the moving element, and the force caused by the change of momentum of water as it hits the base of the moving element of the PRV.

The force terms in Equations (2) and (3) are, from left to right: the net pressure force acting on the both sides of the rolling diaphragms, the spring force due to the deflection of the springs, the friction acting on the moving parts of the controller, and the force caused by change of momentum of water which enters the hole of the hollow and exit from the jet.

Flows through the controller, PRV, and connecting pipes are described using a set of algebraic equations. The flow through the fixed orifice, the needle valve, the pilot valve, and the PRV are given by equations of the form $q = Cv(|\Delta h|)^{1/2}$ sign(Δh) where q, Δh, Cv represent the flow through the element in m^3/s, the pressure loss across the element in metres and the discharge capacitance of the element in m$^{2.5}$/s, respectively and sign (Δh) is the sign of Δh. The discharge capacitance of valve is expressed as a function of the valve opening. The valve discharge capacitance is usually given in the manufacturer's literature for a PRV, and for other elements can be obtained experimentally as described in section 'Experiments to identify component parameters'.

Equation (5) represents the flow through the PRV, where valve discharge capacitance in m$^{2.5}$/s, denoted $Cv_{mv}(x_m)$, depends on valve opening x_m, and is taken from (Prescott & Ulanicki 2003)

$$q_m = Cv_{mv}(x_m)\sqrt{h_{in} - h_{out}} \tag{5}$$

and where

$$Cv_{mv}(x_m) = 0.02107 - 0.0296e^{-51.1322x_m} + 0.011e^{-261x_m}$$
$$- 0.00325e^{-683.17x_m} + 0.0009e^{-399.5x_m}$$

The flow, denoted q_1, through the fixed orifice between the PRV inlet and $t1$ is measured and the discharge capacitance of the fixed orifice, denoted Cv_{fo}, is calibrated using the experimental data of test 1. The flow q_1 is expressed by

$$q_1 = Cv_{fo}\sqrt{h_{in} - h_{cc}} \tag{6}$$

where Cv_{fo} has a constant value of 8.691×10^{-6} m$^{2.5}$/s

The flow q_2 from the control chamber to the jet chamber through the discharge opening of the jet, is measured and the discharge capacitance of pilot valve in m$^{2.5}$/s, $Cv_j(x_r)$, is calibrated against the gap, x_r, using the experimental data of tests 1, 2 and 3. q_2 and $Cv_j(x_r)$ are described as

$$q_2 = Cv_j(x_r)\sqrt{h_{cc} - h_{cj}} \tag{7}$$

where

$$x_r = (x_{sh1} - x_{sh2}) + L_{sh1} + L_{sh2} - (L_{c1,2} + L_{c3}),$$
$$L_{c3} = (79.1 + 2.33\, N_{mpadj}) \times 10^{-3},$$
$$Cv_j(x_r) = 0.463 \times 10^{-3}(1 - e^{-0.1073x_r})$$

and where x_{sh1} and x_{sh2} are the displacements of the modulation shaft and the pilot shaft, respectively. L_{sh1}, L_{sh2}, $L_{c1,2}$, and L_{c3} are the lengths of the modulation shaft, the pilot shaft, the fixed and the variable lengths of the controller sections measured in metres, respectively. L_{c3} depends on the controller set point (number of opening turns of the main pressure adjuster, N_{mpadj}), and is measured for each experiment setting.

The flow through the bi-directional needle valve q_3, has two different representations depending on the direction of flow which can be either from or to the valve control space. If flow is going out of the control space of the PRV during the valve opening, q_3 in m^3/s is represented by

$$q_3 = Cv_{nv}(n)\sqrt{|h_{cc} - h_{vc}|}\cdot\text{sign}(h_{cc} - h_{vc}) \tag{8}$$

where

$$Cv_{nv}(n) = (0.007753n^4 - 0.1178n^3 + 0.5357n^2$$
$$- 0.1107n - 0.01519) \times 10^{-5} \tag{9}$$

Equation (9) describes the relation between opening turns n of the needle valve, and the valve discharge capacitance in m$^{2.5}$/s, Cv_{nv}, which is taken from (Prescott & Ulanicki 2003). The bi-directional needle valve has a physical limit to deliver the flow from the control space of the PRV, which is defined as the valve saturation flow, denoted $q_{3,sat}$, (Choudhury *et al.* 2008) and is represented by

$$q_{3,sat}(n) = (0.02636n^4 - 0.3574n^3 + 1.473n^2$$
$$- 0.01926n - 0.05029) \times 10^{-5} \tag{10}$$

In the case of the flow going into the PRV control space during PRV closure, the needle valve discharge capacitance is constant and equal to 0.11×10^{-3} m$^{2.5}$/s. The characteristics of the valve show that the valve closes faster than it opens.

The same flow, q_3, can also be calculated from Equation (4) as a function of displacement x_m

$$q_3 = \frac{\dot{x}_m}{3700(0.02732 - x_m)} \tag{11}$$

Flow q_6, into the jet chamber through the modulation adjuster, measure in m^3/s is described by Equation (12), the modulation adjuster is a one-directional (into the jet chamber direction) needle valve, and the flow is present if the pressure at $t2$ (h_{t2}) is higher than the pressure in the jet chamber (h_{cj}), otherwise the valve is closed. Discharge capacitance of the modulation adjuster, $Cv_{ma}(n)$ was calibrated using the results of test a for different numbers of opening, n, and is valid for $0 \leq n \leq 8$.

$$q_6 = Cv_{ma}\sqrt{|h_{t2} - h_{cj}|}\cdot\text{sign}(h_{t2} - h_{cj}) \tag{12}$$

where

$$Cv_{ma} = 10^{-4}[2.371 - 2.4240\cos(0.5015n)$$
$$- 1.814\sin(0.5015n) - 0.2775\cos(1.0030n)$$
$$+ 1.230\sin(1.0030n) + 0.3311\cos(1.5045n)$$
$$- 0.1315\sin(1.5045n)]$$

The relation between the pressure drop and flow q_4, measured in m^3/s through the pipe between the Pitot tube and $t2$, is described by the Darcy–Weisbach formula given in Equation (13)

$$h_{out,t} - h_{cpt} = f_4\frac{L_4}{D_4}\frac{1}{2g}\left(\frac{q_4}{A4}\right)^2 \tag{13}$$

where the total pressure, denoted $h_{out,t}$, is equal to the PRV outlet pressure plus the dynamic pressure in the Pitot tube. L_4, D_4, A_4, and f_4 are the length, the diameter in metres, the internal cross sectional area in m^2 and the friction coefficient of the connecting pipe.

The equation can be re-arranged to obtain q_4

$$q_4 = A_4\sqrt{2g\frac{D_4}{f_4 L_4}}\sqrt{h_{out,t} - h_{cpt}} \tag{14}$$

where

$$h_{out,t} = h_{out} + \frac{1}{2g}\left[\left(\frac{q_m}{A_{mv,out}}\right)^2 - \left(\frac{q_4}{A_{Pitot}}\right)^2\right]$$

Finally, the flow from/to the Pitot chamber can be calculated from change in the volume of the Pitot chamber, as shown in Equation (15)

$$q_5 = \dot{x}_{sh1}A_1 \tag{15}$$

The mass balance Equations (16) and (17) for junctions $t1$ and $t2$, respectively, complete the algebraic part of the model

$$q_1 + q_3 = q_2 \tag{16}$$

$$q_5 + q_6 = q_4 \tag{17}$$

The pump characteristic has been estimated from the test rig measurements, and the delivered pressure, h_{in}, can be expressed as a cubic function of the main flow

$$h_{in} = -0.026 \times 10^9 q_m^3 + 0.3562 \times 10^6 q_m^2 - 1.8605 \\ \times 10^3 q_m + 77.947 \tag{18}$$

where q_m is in m^3/s and h_{in} in metres.

The described model can be simplified by ignoring the inertia and friction terms (the second and first derivatives of x) in Equations (1)–(3). The model can be further simplified by ignoring the pressure drops in the short connecting pipes and assuming that $h_{t1} = h_{cc}$, $h_{t2} = h_{cpt}$, and $h_{cj} = h_{out}$. In this paper during simulations the friction terms in the model were ignored.

STRUCTURE OF THE MODEL

In order to better understand the mathematical structure of the model, the formal state space notation is introduced. Define the state vector $\mathbf{x}$, the vector of algebraic variables $\mathbf{y}$ and the vector of parameters $\boldsymbol{\mu}$ as follows.

$$\mathbf{x} = \begin{bmatrix} x_1 \\ x_2 \\ x_3 \\ x_4 \\ x_5 \\ x_6 \end{bmatrix} = \begin{bmatrix} x_m \\ \dot{x}_m \\ x_{sh1} \\ \dot{x}_{sh1} \\ x_{sh2} \\ \dot{x}_{sh2} \end{bmatrix}, \quad \mathbf{y} = \begin{bmatrix} y_1 \\ y_2 \\ y_3 \\ y_4 \\ y_5 \\ y_6 \\ y_7 \\ y_8 \\ y_9 \\ y_{10} \\ y_{11} \\ y_{12} \\ y_{13} \end{bmatrix} = \begin{bmatrix} h_{out} \\ h_{vc} \\ h_{cpt} \\ h_{cj} \\ q_1 \\ q_2 \\ q_3 \\ q_4 \\ q_5 \\ q_6 \\ x_r \\ Cv_j \\ h_{out,t} \end{bmatrix},$$

$$\boldsymbol{\mu} = \begin{bmatrix} \mu_1 \\ \mu_2 \\ \mu_3 \\ \mu_4 \\ \mu_5 \\ \mu_6 \\ \mu_7 \\ \mu_8 \\ \mu_9 \\ \mu_{10} \\ \mu_{11} \\ \mu_{12} \\ \mu_{13} \\ \mu_{14} \\ \mu_{15} \\ \mu_{16} \\ \mu_{17} \\ \mu_{18} \\ \mu_{19} \\ \mu_{20} \\ \mu_{21} \\ \mu_{22} \\ \mu_{23} \end{bmatrix} = \begin{bmatrix} \rho \\ g \\ a_1 \\ a_2 \\ m_m \\ m_{sh1} \\ A_1 \\ k_{sp1} \\ A_j \\ m_{sh2} \\ A_2 \\ k_{sp2} \\ q_m \\ h_{in} \\ Cv_{mv} \\ Cv_{fo} \\ L_{C3} \\ Cv_{nv} \\ q_{3,sat} \\ Cv_{ma} \\ k_4 \\ A_{mv,out} \\ A_{Pitot} \end{bmatrix} \tag{19}$$

The additional relationships between state variables can be derived from the definition above.

$$\dot{x}_1 = x_2 \tag{20}$$

$$\dot{x}_3 = x_4 \tag{21}$$

$$\dot{x}_5 = x_6 \tag{22}$$

The general structure of the model can be represented by a vector differential algebraic equation.

$$\begin{cases} \dot{x}(t) = \mathbf{f}(\mathbf{x}(t), \mathbf{y}(t), \boldsymbol{\mu}) \\ \mathbf{g}(\mathbf{x}(t), \mathbf{y}(t), \boldsymbol{\mu}) = 0 \end{cases} \tag{23}$$

There are six state equations; the first equation is defined by Equation (20), the second by Equation (1), the third by

Equation (21), the fourth by Equation (2), the fifth by Equation (22) and finally the sixth by Equation (3). The algebraic part $\mathbf{g(x,y,\mu)}$ is defined by Equations (4)–(18) excluding Equation (13).

Singularity in the model

Initially the model was implemented in Matlab but despite trying many different solvers the simulations failed to converge and consequently it was decided to use the Mathematica package. In order to accomplish a better understanding of the PRV behaviour and to identify numerical problems encountered in the simulation a simplified problem has been solved analytically (in steady-state conditions and without the outlet pressure modulation).

Equation (1) in steady-state condition becomes

$$\rho g[h_{in}a_1 + h_{out}(a_2 - a_1) - h_{vc}a_2] - m_m g + \rho \frac{q_m^2}{a_1} = 0 \qquad (24)$$

Moreover $h_{cc} = h_{vc}$, $q_3 = 0$ and $q_5 = 0$, hence $q_1 = q_2$ and $q_4 = q_6$. In the steady state x_r is constant and subsequently $Cv_j(x_r)$ is constant too. Then from Equations (5) and (6)

$$h_{vc} = \beta_1 h_{in} + \beta_2 h_{out} \qquad (25)$$

where

$$\beta_1 = \frac{Cv_{fo}^2}{Cv_{fo}^2 + Cv_j^2} \text{ and } \beta_2 = \frac{Cv_j^2}{Cv_{fo}^2 + Cv_j^2},$$

which confirms that the pressure in the control space of the PRV is a convex combination of the inlet and outlet pressures.

Substituting h_{vc} from (24) to (25) allows us to evaluate h_{out}

$$h_{out} = h_{in} - \frac{\left(\frac{m_m}{a_1\rho}\right) - \left(\frac{q_m^2}{a_1^2 g}\right)}{\left(1 - \frac{a_2}{a_1}\beta_1\right)} \qquad (26)$$

The value of β_1 depends on the discharge capacitance and it can happen that the term $(1 - \frac{a_2}{a_1}\beta_1)$ is close to zero causing a singularity in Equation (26) as depicted by the plot in Figure 7. The singularity happens for $\beta_{1,\text{critical}} = a_1/a_2$. The branch of the plot for $\beta_1 < \beta_{1,\text{critical}}$ represents the physical situation when the outlet pressure is smaller than the inlet

pressure, while the branch of the plot for $\beta_1 > \beta_{1,\text{critical}}$ is just a mathematical construct. The value of h_{out} tends to $-\infty$ just before $\beta_{1,\text{critical}}$ and rises to $+\infty$ just after $\beta_{1,\text{critical}}$. If a numerical solver starts with an initial guess corresponding to $\beta_1 > \beta_{1,\text{critical}}$ it may fail to converge to a physical solution, which probably was the reason for the failure of the Matlab simulations.

RESULTS AND DISCUSSION

Steady state results

A number of steady-state characteristics have been measured as an initial assessment of the functionality and robustness of the AQUAI-MOD® hydraulic controller. The corresponding mathematical model was solved using the Mathematica software package and subsequently compared with the measurements to validate the developed mathematical model. In particular, the effects of the flow modulation adjuster and the main pressure adjuster were investigated in steady state to evaluate the performance of the controller.

Modulation adjuster effect

Figure 8 depicts a family of the modulation curves for different settings of the modulation adjuster and for fixed
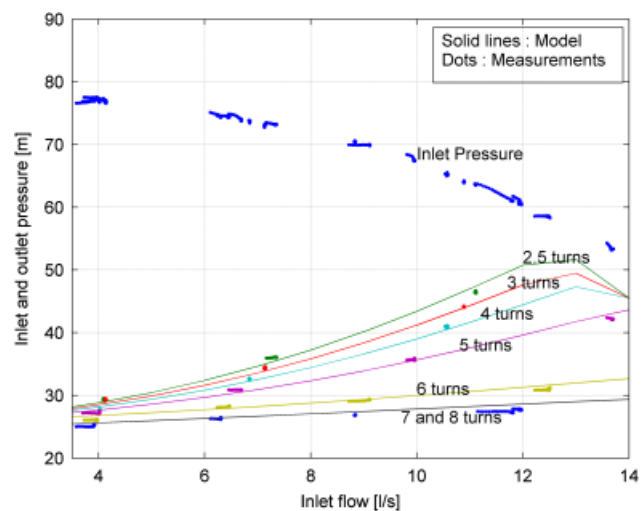

Figure 8 | Modulation curve of the AQUAI-MOD® controller at different setting of modulation adjuster and 6.5 opening turns of main pressure adjuster.
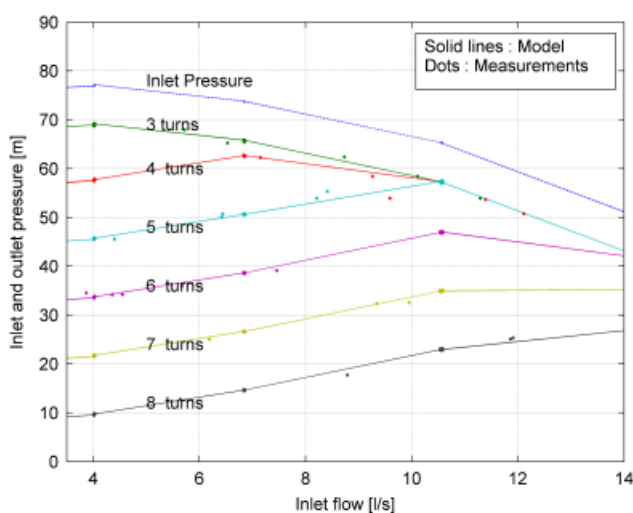
6.5 opening turns of the main pressure adjuster (test 1 and 2). The solid lines represent results from the model and the coloured patches represent noisy measurements. It can be observed that when the main flow increases the outlet pressure of the PRV increases confirming the flow modulation effect. The pressure drop at high flows is due to the test rig arrangement, that is the PRV inlet pressure decreases due to the pump characteristics. The modulation effect is more prominent for almost closed modulation adjuster. The effect of the modulation almost disappears for the almost fully opened adjuster.

Main pressure adjuster effect

Figure 9 shows a family of the modulation curves for different number of opening turns of the main pressure adjuster (test 4) again the solid lines represent results from the model and the coloured patches represent noisy measurements. It can be observed that settings in range of zero to three turns have no effect, and the outlet pressure stays almost constant, which means that the PRV is fully open. More turns correspond to a lower 'minimum pressure set point', for each opening turn the modulation curve shifts down by 12 m as it can be observed.

Typical operating condition in steady state

The steady-state model is validated by comparing the results of the model and experimental data during different regimes

of the valve operation in a typical operating condition of both the inlet flow and pressure. The experimental main flow and the inlet pressure are used as given inputs to the mathematical model. In all cases the steady state model results show a good agreement with the experimental data in trends and magnitudes. Figure 10 shows the experimental inlet flow, the inlet pressure and the outlet pressure as well the results of the steady state mathematical model. In this case, the minimum pressure is set by the main pressure adjuster (6.5 opening turns) to 26 m corresponding to the minimum flow of 1.85 l/s, and the maximum pressure is set by the main modulation adjuster (four opening turns) to 41.5 m corresponding to the flow of 10.6 l/s. Minimum and maximum flow rate are chosen to be in the normal operating range for the PRV. A very good agreement between the experimental and model output pressure is observed with relative root mean squared error of 0.090.

Dynamic results

The mathematical model including the dynamic aspects were solved using the Mathematica software package to evaluate the behaviour of the system for varying main valve flow. The results of the mathematical model were compared with the experimental data obtained from the test rig to validate the model in dynamic conditions. The results of the full model were compared with the experimental data, and showed a
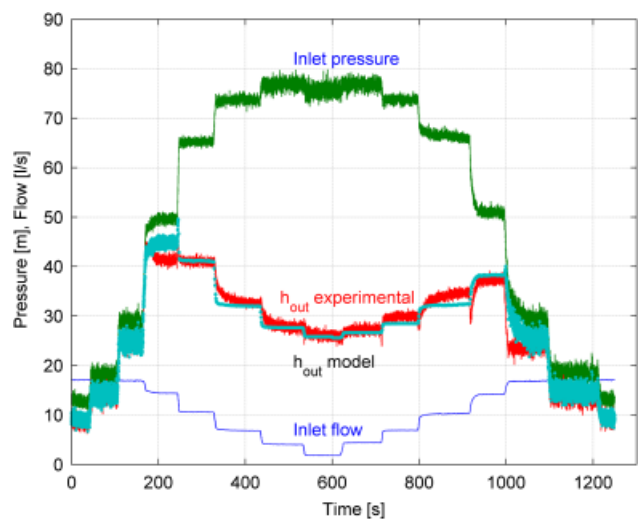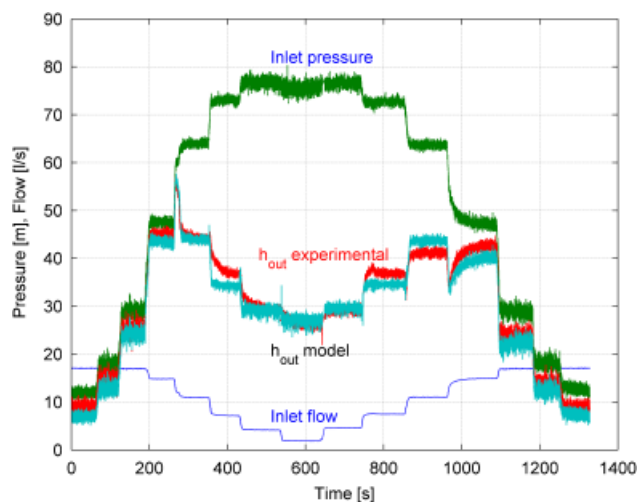

Figure 9 | Modulation curve of the AQUAI-MOD® controller at different setting of main pressure adjuster and four opening turns of modulation adjuster.

Figure 10 | Steady-state model results compared with experimental data for step decreasing followed by step increasing of inlet flow.
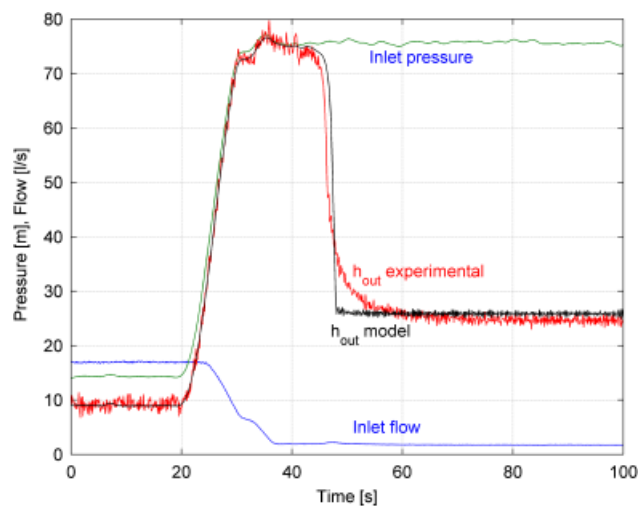
Figure 11 | Results of dynamic model compared with experimental data for stepping the inlet flow down and up.

Figure 12 | Results of dynamic model compared with experimental data of sharp closure, with three opening turns of modulation adjuster and 6.5 of main pressure adjuster.

good agreement in the values and trends, as shown in Figure 11, for a typical operating condition in terms of flow and inlet pressure, with the modulation adjuster set up to three turns and the main pressure adjuster to 6.5 turns. These settings correspond to the minimum pressure of 26 m (minimum flow of 1.85 l/s), and the maximum pressure of 45 m (flow of 11 l/s). The relative root mean squared error between the results from the model and the experimental data has a value of 0.100.

Figure 12 shows the results of the dynamic model compared with experimental data for a sharp closure of the downstream gate valve with the modulation adjuster set up to three turns and the main pressure adjuster to 6.5 turns as described in test 4. The mathematical model does not consider water hammer in the pipes of the system. Note that the closure of the downstream gate valve is not sufficiently fast to show any water hammer effects. Both experiment and the numerical results show a good agreement in both trend and magnitude, and have an error of 0.080 in terms of relative root mean squared error.

In Figure 12 there is a difference between the measured and simulated outlet pressures for $t = 47$ s. The measured pressure decreases at a slower rate and this is probably due to the simplifying assumptions ignoring friction forces.

It was observed from both experiments and modelling studies that the dominant dynamic behaviour of the PRV equipped with the AQUAI-MOD® controller is decided by the movement of the PRV main element and is the same as a standard PRV with a pilot valve.

CONCLUSIONS

The AQUAI-MOD® hydraulic controller is a device to control and modulate the outlet pressure of a PRV according to the valve flow. The modulation curve is defined by the set points for the minimum and maximum outlet pressure corresponding to the minimum and maximum flow, respectively. The controller has been experimentally tested via carefully designed experiments to assess its performance and functionality in different conditions and operating ranges. The controller in all cases has showed a good performance by modulating the outlet pressure between the minimum and maximum set points as expected. The dynamic behaviour of the valve has also been tested and presented, followed by a detailed explanation. The controller has worked as expected in all tested conditions and it was found that the dominant dynamic behaviour of the PRV equipped with the AQUAI-MOD® controller is the same as a standard PRV with a pilot valve. It is considered that such hydraulic flow-modulated devices could be used to reduce the leakage while satisfying pressure requirements.

The mathematical model of the controller has been developed and solved with the Mathematica software package for

both steady-state and dynamic conditions. The results of the model have been compared with the experimental data and showed a good agreement in the magnitude and trends. The developed models can be used to compute the required adjustment for the minimum and maximum pressure set points before installing the controller in the field, or to simulate the behaviour of a PRV and the AQUAI-MOD® hydraulic controller in typical network applications.

It is considered that the experiment design and modelling approach described in this paper can be helpful for other authors developing mathematical models of similar systems. Such models can be used at the design stage to size the components of a hydraulic controller and to improve its characteristics. They can also be integrated with water network simulators to study the behaviour of water distribution systems governed by hydraulic flow-modulation controllers.

ACKNOWLEGEMENTS

REFERENCES

Alonso, J. M., Alvarruiz, F., Guerrero, D., Hernández, V., Ruiz, P. A., Vidal, A. M., Martínez, F., Vercher, J. & Ulanicki, B. 2000 Parallel computing in water network analysis and leakage minimization. *J. Wat. Res. Plan. Manage.* **126**(4), 251–260.

Andersen, J. H. & Powell, R. S. 1999 Simulation of water networks containing controlling elements. *J. Wat. Res. Plan. Manage.* **125**(3), 162–169.

Brunone, B. & Morelli, L. 1999 Automatic control valve-induced transients in operative pipe system. *J. Hydraul. Engng.* **125**(5), 534–542.

Çakmakcı, M., Uyak, V., Öztürk, İ., Aydın, A. F., Soyer, E. & Akça, L. 2007 The dimension and significance of water losses in Turkey. *Proceedings of IWA Specialist Conference on Water Loss*, 23–26 September, Bucharest, Romania, pp. 464–473.

Choudhury, A. A. S., Shah, S. L. & Thornhill, N. F. 2008 *Diagnosis of Process Nonlinearities and Valve Stiction*. Springer, Berlin, Heidelberg, New York.

Colombo, A. F. & Karney, B. W. 2009 Impacts of leaks on energy consumption in pumped systems with storage. *J. Wat. Res. Plan. Manage.* **131**(2), 146–155.

Girard, M. & Stewart, R. A. 2007 Implementation of pressure and leakage management strategies on the Gold Coast, Australia: case study. *J. Wat. Res. Plan. Manage.* **133**(3), 210–217.

Marunga, A., Hoko, Z. & Kaseke, E. 2006 Pressure management as a leakage reduction and water demand management tool: The case of the City of Mutare, Zimbabwe. *Phys. Chem. Earth* **31**(15–16), 763–770.

Pérez, R., Martínez, F. & Vela, A. 1993 Improved design of branched networks by using pressure-reducing valves. *J. Hydraul. Engng.* **119**(2), 164–180.

Prescott, S. & Ulanicki, B. 2004 Investigating interaction between pressure reducing valves and transients in water networks. In: Sawodny, O. & Scharff, P. (eds) *Proc. of 49th International Scientific Colloquium*. Technische University, Ilmenau, Shaker, Aachen, Germany, pp. 49–54.

Prescott, S., Ulanicki, B. & Renshaw, J. 2005 Dynamic behavior of water networks controlled by pressure reducing valves. CCWI2005-Water management for the 21st century. In: Savic, D., Walters, G., King, R. & Khu, S. (eds) *Centre for Water Systems*. University of Exeter, Devon, UK, pp. 239–244.

Prescott, S. L. & Ulanicki, B. 2003 Dynamic modeling of pressure reducing valves. *J. Hydraul. Engng* **129**(10), 804–812.

Prescott, S. L. & Ulanicki, B. 2008 Improved control of pressure reducing valves in water distribution networks. *J. Hydraul. Engng.* **134**(1), 56–65.

Rogers, D. 2005 Reducing leakage in Jakarta, Indonesia. *Proceedings of the IWA Specialist Conference: Leakage 2005*, 12–14 September, Halifax, Nova Scotia, Canada.

Thornton, J. & Lambert, A. O. 2007 Pressure management extends infrastructure life and reduces unnecessary energy costs. *Proceedings of IWA Specialist Conference on Water Loss*, 23–26 September, Bucharest, Romania, pp. 511–521.

Ulanicki, B., AbdelMeguid, H., Bounds, P. & Patel, R. 2008 Pressure control in district metering areas with boundary and internal pressure reducing valves. In *Proc. of 10th International Water Distribution System Analysis conference, WDSA2008*. The Kruger National Park, South Africa.

Ulanicki, B., Bounds, P. L. M., Rance, J. P. & Reynolds, L. 2000 Open and closed loop pressure control for leakage reduction. *Urban Water* **2**(2), 105–114.

Vairavamoorthy, K. & Lumbers, J. 1998 Leakage reduction in water distribution systems: optimal valve control. *J. Hydraul. Engng* **124**(11), 1146–1154.

Yates, C. D. & MacDonald, G. D. 2007 Advanced pressure management via flow modulation; the Dartmouth Central PMA. *Proceedings of IWA Specialist Conference on Water Loss*, 23–26 September, Bucharest, Romania, pp. 541–548.